CRYSTAL GROWTH & DESIGN

Article

pubs.acs.org/crystal

Removal of Copper Vacancies in Cuprous Oxide Single Crystals Grown by the Floating Zone Method

Kelvin B. Chang,[†] Laszlo Frazer,[‡] Johanna J. Schwartz,[‡,#] John B. Ketterson,[‡,¶] and Kenneth R. Poeppelmeier*[,†,§]

[†]Department of Chemistry, Northwestern University, 2145 Sheridan Road, Evanston, Illinois 60208

[‡]Department of Physics, Northwestern University, 2145 Sheridan Road, Evanston, Illinois 60208

[¶]Department of Electrical Engineering and Computer Science, Northwestern University, 2145 Sheridan Road, Evanston, Illinois 60208

[§]Chemical Sciences and Engineering Division, Argonne National Laboratory, 9700 South Cass Avenue, Argonne, Illinois 60439

Supporting Information

ABSTRACT: Single crystals of cuprous oxide (Cu_2O) with minimal defects were grown using the optical floating zone technique. Copper vacancies were removed through the promotion of CuO precipitation within the bulk Cu_2O crystal following the reaction $Cu_{Cu}^{Cu_2O} + V_{Cu}^{Cu_2O} + O_O^{Cu_2O} \rightarrow Cu_{Cu}^{CuO} + O_O^{CuO}$. This reaction was promoted through the use of high purity samples and by growing crystals under an oxidizing atmosphere. Although an increase in the oxygen concentration of the atmosphere will initially increase the oxygen to copper ratio, the excess oxygen in the final Cu_2O crystal is ultimately decreased through the formation of CuO as the crystal cools. Copper vacancies were reduced further, and the CuO phase was eventually removed from the Cu_2O crystal when thin slices of the crystal were annealed.

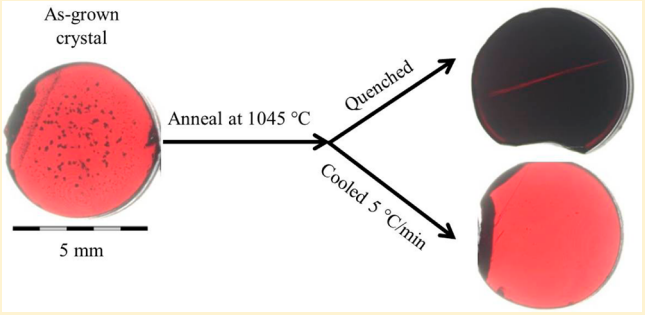

1. INTRODUCTION

Deviation of a material from stoichiometry can impact properties and applications. Cu_2O is a classic example of a cation-deficient material where properties are determined by nonstoichiometry. While copper vacancies and oxygen interstitials could each lead to cation deficiency, the former is the dominant defect in Cu_2O.[1] The copper vacancies dictate a number of characteristics: (1) Cu_2O is a p-type semiconductor.[2] (2) Copper vacancies increase with increasing oxygen pressure,[3,4] resulting in increased conductivity.[5−8] (3) The oxidation of Cu metal to Cu_2O and the oxidation of Cu_2O to CuO occur through the outward migration of copper atoms toward the surface.[9−12] (4) Cuprous oxide exhibits exceptionally long exciton lifetimes of up to 13 μs.[13] Copper vacancies, however, alter the symmetry of excitons, which allow them to decay faster. A sample with optimized conductivity and exciton lifetime cannot be achieved simultaneously. Oxygen vacancies also shorten exciton liftetimes, but copper vacancies are dominant.[14] Therefore, conditions for crystal growth that influence the concentration of copper vacancies in cuprous oxide must be understood in order to obtain optimal samples for the intended purpose.

Our objective in the present work is to grow large cuprous oxide single crystals with minimal copper vacancies to be used in exciton studies. Cuprous oxide has been grown through a variety of methods. Hydrothermal synthetic routes allow for morphology control of nanoparticles.[15−18] Small crystals can be obtained through the thermal oxidation of copper metal.[19,20] Epitaxial films can be grown on MgO from a melt,[21] magnetron sputtering,[22] or thermal oxidation.[23] Techniques that involve growing from a melt are better suited to grow bulk crystals several millimeters in size in all three dimensions. While bulk crystals of many materials are commonly grown from a melt using Bridgeman-like directional solidification[24−28] and Czochralski methods,[29−32] they each require the use of a crucible. A study by Zucker found that molten cuprous oxide is highly reactive with most crucible materials.[33] MgO was found to be a suitable crucible material for the Czochralski crystal growth of cuprous oxide, although some reactivity between MgO and molten cuprous oxide was still observed over extended periods of time.[33] Therefore, the crucible free floating zone method[34,35] is ideal for growing high purity bulk cuprous oxide crystals.

The Cu−O phase diagram indicates that Cu_2O melts congruently in air at approximately 1120 °C.[36,37] Additionally, the phase diagram shows that Cu_2O becomes metastable below 1020 °C, at which point CuO becomes the thermodynamic phase. Nonetheless, the kinetics for Cu_2O oxidation below 1020 °C are sufficiently slow to allow Cu_2O to be grown in

Received: July 17, 2013
Revised: September 24, 2013
Published: October 29, 2013

   dx.doi.org/10.1021/cg401081m | *Cryst. Growth Des.* 2013, 13, 4914−4922

imaging furnaces, as previously reported.[37−41] Single crystals, however, contain CuO inclusions, which can be removed through thermal processing.[37] Ito et al. also examined the effect a number of growth parameters had on copper vacancies.[41] These studies included changing the conditions to prepare Cu_2O rods through thermal oxidation of copper metal. They concluded that oxidizing a copper rod for 4 days at 1045 °C was the optimal oxidation procedure for preparing cuprous oxide rods. The effects of conditions for crystal growth on copper vacancies in the final crystal were examined through the variation of growth rate, rotation rate, and oxygen concentration during crystal growth. They found that a slower growth rate reduced copper vacancies, and varying rotation rate did not have an effect. Lastly, a crystal grown in air contained fewer vacancies than one grown under 3% O_2 in Ar.

Two potential methods to decrease the concentration of copper vacancies in Cu_2O during crystal growth are described here. One potential method to influence copper vacancy concentration is to control the amount of excess oxygen in the crystal. While one may think the amount of oxygen released or introduced into the molten zone could be influenced by the rotation rate of the rods, the rotation rate has previously been shown to have no effect on the copper vacancy concentration.[41] Another way to potentially vary the excess oxygen in the crystal is to use feed rods with different concentrations of copper vacancies. Results presented in this manuscript, however, suggest that an alternative approach to remove copper vacancies is more effective.

A mechanism proposed previously[37] for reducing copper vacancies in cuprous oxide is through the formation of cupric oxide as a secondary phase in the bulk crystal.

$$Cu_{Cu}^{Cu_2O} + V_{Cu}^{Cu_2O} + O_{O}^{Cu_2O} \rightarrow Cu_{Cu}^{CuO} + O_{O}^{CuO} \quad (1)$$

This reaction does not change the overall Cu:O ratio in the sample as a whole. The excess oxygen in the Cu_2O phase is removed by forming CuO within the sample once the sample is cooled into the CuO phase boundary. The oxidation of Cu_2O to CuO begins with the formation of a thin CuO layer on the surface. The bulk of the sample is then oxidized through the outward migration of copper atoms toward the surface.[11,12] Additionally, eq 1 indicates that CuO can precipitate from the Cu_2O lattice without first reaching the CuO surface layer. This mechanism is consistent with the presence of CuO inclusions inside Cu_2O crystals in addition to the CuO surface layer that forms. With this methodology, the copper vacancy concentration can be decreased through the promotion of CuO precipitation as a secondary phase *after* Cu_2O has crystallized from the molten zone. One might expect the oxidizing conditions that promote the formation of CuO to also promote a more oxidized Cu_2O sample (i.e., more copper vacancies). The reaction in eq 1, however, is consistent with the fact that lower temperatures within the Cu_2O region of the phase diagram (approaching the CuO phase boundary) result in fewer copper vacancies.[14]

CuO formation can be promoted if the activation energy for the oxidation of cuprous oxide is lowered. A study by Zhu et al. showed that the presence of impurities can inhibit CuO growth.[11] They found at temperatures below 950 °C, a low purity sample has a higher activation energy for oxidation than a high purity sample. This difference is largest between 800 and 950 °C. Other studies have also shown that the activation energy for the oxidation of Cu_2O is significantly lowered (even negative) at higher temperatures, above approximately 800 °C.[11,42,43] Therefore, copper vacancies should be reduced if higher purity starting materials are used and if the crystal is maintained at kinetically relevant temperatures for longer periods of time. The latter point could be achieved through: (1) an increase in the temperature of the Cu_2O-CuO phase boundary by increasing oxygen pressure, (2) an increase in temperature of the sample below the molten zone, and (3) a slower growth rate. This strategy is counterintuitive as it promotes the formation of a secondary phase, while previous methods for obtaining Cu_2O crystals involve cooling under a vacuum or using an inert atmosphere to inhibit CuO formation.[20,33,37,39,40] Several cuprous oxide crystals were grown in a floating zone optical imaging furnace to examine how the conditions for crystal growth listed above can be varied to reduce the number of copper vacancies.

Postgrowth annealing experiments were also performed to determine the role of annealing in the formation of copper vacancies. When these image-furnace grown crystals are annealed in the Cu_2O region of the phase boundary, CuO will reduce to Cu_2O and incorporate additional copper vacancies through the reverse of eq 1. The cooling rate will dictate how many vacancies are removed through the formation of CuO upon cooling. If the samples are quenched, CuO formation is minimized, which will result in a higher concentration of copper vacancies when compared to the original sample. Similarly, samples cooled more slowly will contain fewer copper vacancies.

2. EXPERIMENTAL SECTION

2.1. Cu_2O Rod Preparation. Feed and seed rods were prepared through the thermal oxidation of copper metal rods. Three different purity ratings of copper were used. 99.9% pure copper rods were purchased from the Industrial and Scientific Department of Amazon. 99.99% pure copper rods were purchased from McMaster-Carr. 99.999% pure copper rods were purchased from Alfa Aesar. 99.9% pure rods both 4.76 and 6.35 mm in diameter were used. The 99.99% pure copper rods were 6.35 mm in diameter. The 99.999% pure copper rods were 5.0 mm in diameter. The radial temperature gradient is dependent on the diameter of the rod. For experiments in which the purity of the sample was varied, crystals were grown from copper rods 5 mm in diameter to maintain a constant temperature gradient. Larger crystals, however, are easier to process. Therefore, copper rods 6.35 mm in diameter were used in experiments in which a different temperature gradient was less critical.

While holes are often drilled to thread wires to suspend the feed rod in the imaging furnace, holes could not be easily drilled into the rods after oxidation without breaking the rod. Holes drilled in the copper metal rods before oxidation were filled from expansion of the material during oxidation. A groove was instead machined into one end of the metal rod prior to oxidation. These grooves were still present after oxidation and allowed the feed rods to be wrapped with wire to hang in the furnace. The rods were etched in 1 M HCl for approximately 1 h followed by washing with water to clean the surface prior to oxidation.

Based purely on the phase diagram, cuprous oxide crystals could be grown using copper metal for the feed and seed rods. The high thermal conductivity of copper metal, however, can prevent concentrated heating needed to form the molten zone.[41] Copper rods were therefore oxidized to Cu_2O in a furnace for 3 days at 1045 °C to be used as seed and feed rods. At elevated temperature, cuprous oxide will react with normally inert materials, including platinum.[37] To minimize contamination, V-shaped supports made from copper foil were placed along the entire length of an inverted alumina boat. Copper rods were then placed on top of the foil supports. Using this method, copper foil is the only material in contact with the copper rods and contamination is minimized. The 99.9% and 99.99% rods

dx.doi.org/10.1021/cg401081m | Cryst. Growth Des. 2013, 13, 4914−4922

were supported with 99.9% pure, 0.127 mm thick copper foil (Alfa Aesar). The 99.999% pure rods were supported with 99.9999% pure copper foil. After oxidation, a thin layer of CuO formed on the surface of the rods. The CuO layer was removed by etching the rods in 1 M nitric acid for a few hours and washing with water, followed by physical etching with sandpaper. The density of the final Cu_2O rod was measured to be about 95% of the calculated crystal density.

2.3. Crystal Growth. Crystals were grown in an optical image furnace (CSI FZ-T-10000-H-VI-VP) equipped with four 300 W tungsten halide lamps. Each lamp is positioned in an elliptical mirror to focus light on a narrow portion of the sample. Feed rods were suspended from the upper shaft using steel wire. Seed rods were mounted to the bottom shaft using an alumina chuck and were anchored with steel wire. Feed and seed rods were enclosed in a fused silica tube to allow for atmospheric control. The furnace is equipped with two gas inlets with independent flow rate controls to allow for gas mixing. Oxygen and argon gas tanks were connected to control the oxygen concentration. The furnace is also equipped with a pump that can provide an atmospheric air flow into the growth chamber. The initial copper vacancy concentration of feed rods, rotation rate, sample purity, oxygen content of the atmosphere, lamp power, and growth rate were varied as described below. Unless otherwise stated, samples were grown in air at a rate of 7.0 mm/h with the feed and seed rods rotating at 7 rpm in opposite directions.

2.4. Annealing of Crystals. A crystal grown was from a 99.9% pure copper rod 4.76 mm in diameter. This crystal was cut into 10 slices approximately 1 mm thick perpendicular to the direction of growth. Each slice was placed on an inverted alumina crucible. Slices were supported by two pieces of Cu_2O foil to prevent contamination from the crucible. The Cu_2O foil was produced from the oxidation of copper metal foil and was obtained from the foil to support copper rods during the initial oxidation procedure described above. All samples were annealed in air in a furnace at 1045 °C. Four samples were quenched by removing them from the furnace at 1045 °C and were allowed to cool in air to room temperature after annealing times of 1−4 days at 1 day intervals. Samples reached room temperature within 10 min. Similarly, five samples were cooled to room temperature at a rate of 5 °C/min with annealing times of 1−5 days at 1 day intervals. One slice was not annealed as a control.

2.5. Powder X-ray Analysis. Powder X-ray diffraction patterns were collected using a Rigaku Geigerflex D/MAX-IA diffractometer using Cu Kα radiation with a Ni filter.

2.6. Photoluminescence. Relative concentrations of copper vacancies in the crystals were determined through photoluminescence. A peak in luminescence near 910 nm has been well established to originate from the presence of copper vacancies.[44−46] A typical spectrum is given in the Supporting Information (Figure S1). Cuprous oxide samples were sliced and polished, ultimately with a 1 μm diamond suspension and Buehler MicroCloth textile. The crystallographic orientation of the face does not influence the measurement. Crystals that were grown under constant conditions had slices cut perpendicular to the growth axis. Crystals grown with incremental changes in a given variable during crystal growth were sliced along the growth axis.

Samples were illuminated using a Nd:YVO_4 frequency doubled 532 nm continuous wave laser. Luminescence data were collected at room temperature using off-axis detection through a line filter which removed scattered laser light. A spectrometer with a CCD detector was used to integrate the luminescence from 909 to 920 nm,[44−46] the region where copper vacancy signal is collected most efficiently considering the luminescence spectrum and instrument sensitivity.

For samples that were grown under fixed conditions, a cross-sectional slice was cut from the center of the rod. Measurements were taken at five arbitrary locations on this slice in order to evaluate sample homogeneity. For samples grown with incremental changes in a given variable during the course of crystal growth, the crystal was sliced along the direction of growth. Measurements were taken along the growth axis. These samples were divided into two or three segments. Measurements taken at the edge between segments were removed so photoluminescence plots from segments belonging to the same sample could be merged onto a single plot for clarity. While the measurements were merged, luminescence from the different segments is differentiated by the color of the plotted line. Uncertainties in optical measurements were negligible compared to sample inhomogeneity.

Power dependent luminescence experiments were performed to ensure that the luminescence from the copper vacancies was not saturated. Measurements were made on the sample that showed the highest copper vacancy luminescence. A linear dependence between laser power and luminescence was observed. Luminescence spectra are presented in the Supporting Information (Figure S2).

3. RESULTS AND DISCUSSION

3.1. Deviation from Stoichiometry in the Feed Rod. The effect of the amount of excess oxygen in the initial feed rod on the copper vacancy concentration of the final crystal was examined. Single crystals grown in the floating zone furnace contain significantly fewer copper vacancies than the polycrystalline feed rods. A second growth cycle that used a single crystal as the feed rod was used to determine whether the copper vacancy concentration of the initial feed rod influences the copper vacancy concentration of the final crystal. The following sample was obtained from a 99.99% pure copper rod as the starting material. A single crystal 25 mm long was grown on a seed rod 50 mm long. The single crystal rod was rehung inverted in the furnace and underwent a second crystallization cycle. Once the entire portion of the feed rod that was a single crystal was allowed to recrystallize, growth was continued in order to melt and crystallize the polycrystalline rod that was used as the seed during the first growth cycle. This process resulted in a single rod that contained two portions: one grown from a single crystal and one grown from a polycrystalline rod. The sample was sliced along the growth axis, and photoluminescence was measured along the entire sample. The integrated copper vacancy intensity is plotted against the position along the crystal in Figure 1. Sections of the sample grown from the single crystal and polycrystalline rod are highlighted in green and blue, respectively. No clear difference exists that would indicate an initial feed rod with fewer copper vacancies would yield a single crystal with lower copper vacancies. This suggests that the copper−oxygen ratio reaches

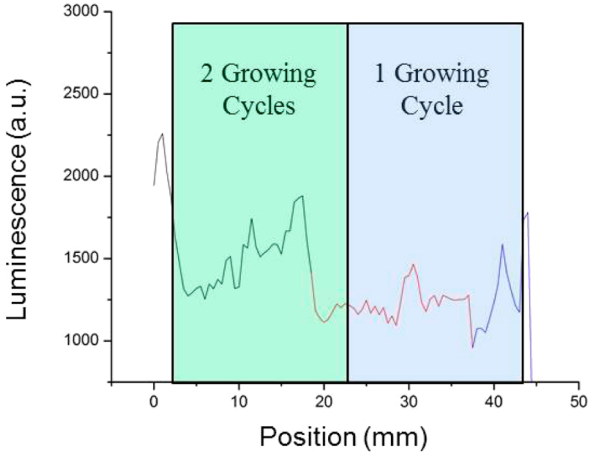

Figure 1. Copper vacancy luminescence along the growth axis of a Cu_2O crystal. The green box represents the portion of the sample that was grown from a single crystal feed rod. The blue box represents the portion of the sample that was grown from a polycrystalline feed rod. The black, red, and blue coloring of the line represents different segments of the same crystal from which the measurement was taken.

equilibrium during the growth process, regardless of the copper vacancy concentration of the initial rod.

3.2. Varying Rotation Rate. A crystal grown was from a 99.9% pure copper rod 6.35 mm in diameter. The effect of counter-rotation rates on copper vacancy concentration was examined by incrementally increasing the rotation rates along a single sample. Counter-rotation rates were varied from 7 to 70 rpm per rod in five increments with an increase of about 16 rpm per increment. It should be noted that alignment of the feed and seed rods is particularly crucial for high rotation rates, as misalignment can lead to disconnection of the molten zone. Approximately 7 mm were grown at each incremental rotation rate before the rotation rate was changed. Through this method, rotation rate becomes a function of position along the growth axis crystal. Integrated copper vacancy photoluminescence along the growth axis is plotted in Figure 2. The changes

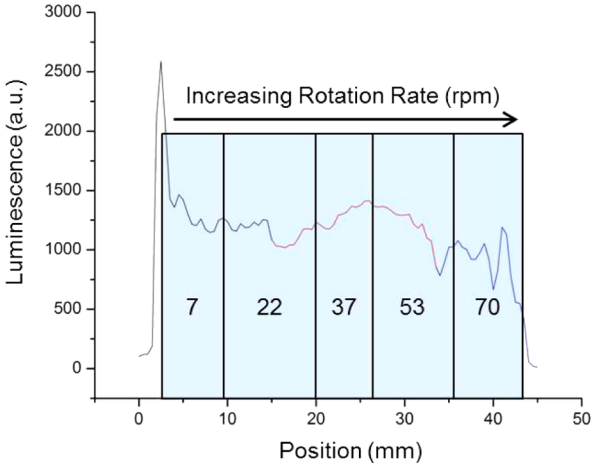

Figure 2. Copper vacancy luminescence along the growth axis of a single Cu_2O sample grown with incrementally increasing counter-rotation rates per rod of feed and seed rods. Rotation rates (rpm) of crystal segments are labeled in blue boxes. The black, red, and blue coloring of the line represents the different segments of the same crystal from which the measurement was taken.

in rotation rates are labeled in blue boxes. No effect from varying rotation rate on copper vacancy formation is observed, consistent with the work from Ito et al.[41] The rotation rate does not influence the equilibrium excess oxygen of the molten zone and final crystal.

3.3. Varying Copper Purity. Three crystals with different purities were grown under otherwise identical conditions. A 99.9% pure sample was grown from the 4.76 mm diameter rod to closely match the diameter of the 5.0 mm 99.999% copper rod. The 99.99% pure rod was machined from 6.35 mm to 5 mm in diameter for the same reason. A slice from each crystal was cut perpendicular to the direction of growth. The copper vacancy luminescence intensity was measured at several positions on each sample. Intensities are given in Figure 3, which indicates that higher purity samples contain fewer copper vacancies. This result is consistent with the fact that impurities can raise the activation energy for oxidizing Cu_2O to CuO.[11] Higher purity favors the removal of copper vacancies through eq 1.

Floating zone crystal growth may result in a purification of the crystal during growth owing to the zone refining effect. The fact that higher purity samples contain fewer copper vacancies luminescence with increasing sample purity would therefore

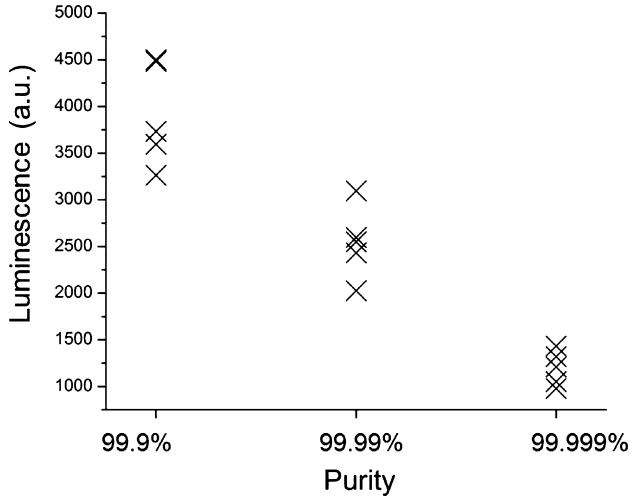

Figure 3. Copper vacancy luminescence for three Cu_2O crystals of varying purity.

suggest that copper vacancy luminescence may decrease along the direction of crystal growth. The luminescence data in Figure 1, however, shows that the copper vacancy luminescence does not decrease as a function of position nor through a second refinement cycle. These results suggest that any purification that does result from zone refining is not significant enough to affect the copper vacancy during the course of crystal growth.

3.4. Oxygen Concentrations of Growth Atmosphere. A crystal approximately 35 mm long was grown from a 99.9% pure copper rod 6.35 mm in diameter. The oxygen concentration of the atmosphere was varied incrementally during the course of crystal growth. The first 7 mm of the crystal were grown under flowing argon. The oxygen concentration in the silica tube was incrementally increased through adjustment of the flow rate of oxygen and argon. The total flow rate was kept constant. As the oxygen concentration increases, however, the melting point of cuprous oxide decreases to an extent that the power of the lamps had to be constantly adjusted accordingly. The rod was sliced along the growth axis. Photoluminescence was measured along the entire sample and is plotted in Figure 4a. The incremental increase in oxygen concentration during the course of sample growth is labeled in blue boxes. Oxygen concentrations are labeled as the percent of oxygen flow rate from the total gas flow.

Figure 4a reveals a general trend that increasing oxygen concentration decreases copper vacancies in the sample, with a sharp drop in luminescence between 0 and 12% oxygen. Because the power applied to the lamps was constantly adjusted, individual crystals were also grown, each under a constant flowing atmosphere at a given oxygen concentration, to study the effect of oxygen concentration on crystals grown with a more stable molten zone. No significant difference in copper vacancy concentrations between samples grown in air, 32%, and 50% oxygen concentration levels were observed. However each of these samples contained fewer copper vacancies than the sample grown under argon. Luminescence data for these samples are given in Figure 4b. The presence of oxygen plays an important role in the formation of copper vacancies. On the basis of Figure 4a,b, however, no additional changes occur in oxygen concentrations between 12 and 50%. Growing samples in air is therefore a suitable atmosphere for

dx.doi.org/10.1021/cg401081m | Cryst. Growth Des. 2013, 13, 4914−4922

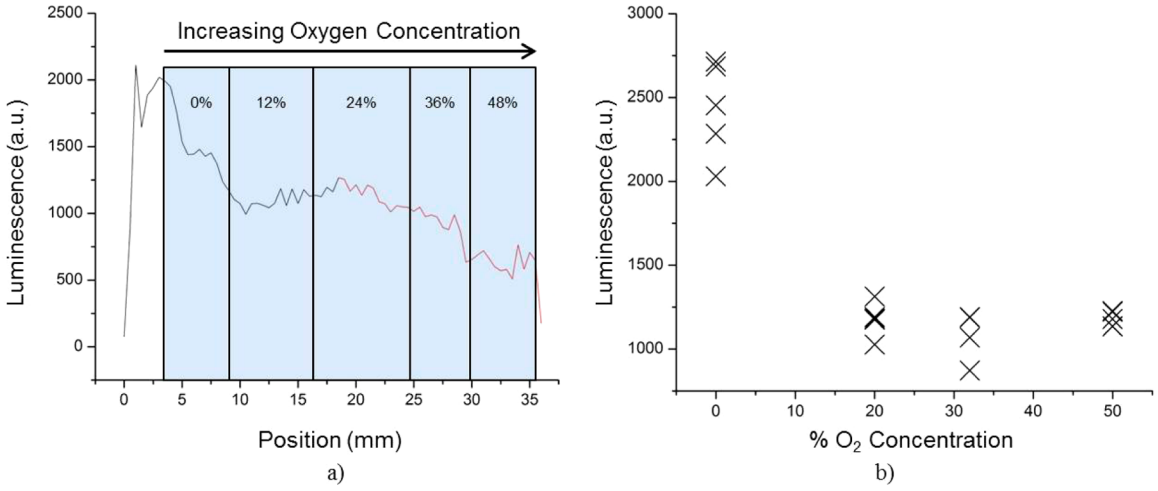

Figure 4. (a) Copper vacancy luminescence along the growth axis of a single Cu_2O sample grown with incrementally increasing oxygen concentrations. Oxygen concentrations of crystal segments are labeled in blue boxes. The black and red coloring of the line represents different segments of the same crystal from which the measurement was taken. (b) Copper vacancy luminescence of four different crystals grown under varying oxygen concentrations.

obtaining crystals with low copper vacancy concentrations. The overall decrease in luminescence intensity observed in Figure 4a from regions grown under 12% to 48% oxygen may be due to the instability of the molten zone caused by the change in melting point. It is important to note that the intensity units between Figure 4a and Figure 4b are arbitrary units and cannot be directly compared to each other.

The fact that a more oxidizing environment lowers copper vacancy concentration may initially seem counterintuitive. One might expect that a more oxidizing environment would oxidize the sample, thereby increasing the number of copper vacancies. As illustrated in the Cu−O phase diagram, however, as oxygen pressure increases, the temperature of the Cu_2O-CuO phase boundary also increases.[36,37] This temperature increase can affect the amount of oxidation that occurs within the floating zone furnace. If the crystal crosses into the CuO region of the phase diagram at a higher temperature, a greater amount of CuO can precipitate and remove vacancies through eq 1. If the sample can oxidize for a longer period of time by crossing into the CuO region at temperatures where the activation energy for oxidation is low, additional copper vacancies are removed from the crystal. The partial pressures of oxygen at the 12−50% oxygen concentrations are at similar levels when viewed on the logarithmic scale presented in the Cu−O phase diagram.[36,37] The temperature at which the crystal crosses into the CuO phase boundary for these oxygen concentrations will therefore be similar, which explains why all these samples contain similar levels of copper vacancies. Growth under higher oxygen concentrations was attempted, but an observed decrease in surface tension and increase in wetting of the molten material on the solid prohibited crystal growth under higher oxygen concentrations.

3.5. Varying Lamp Power. The melting point of Cu_2O decreases with increasing oxygen partial pressure. Samples grown under higher oxygen concentrations are generally grown at a lower temperature, which may influence the number of copper vacancies that are removed via eq 1. To determine whether the growth temperature, influenced by power applied to the lamps, can be raised in the floating zone furnace to promote copper vacancy removal, three crystals made from 99.99% pure copper rods were grown at different temperatures by varying the voltage and current applied to the lamps. A slice was cut from each of the three samples. The copper vacancy luminescence was measured several times for each sample. These measurements are presented in Figure 5. The 56.8% power level represents the lowest possible power that could be used to melt and grow a crystal in the furnace. The 60.8% power level represents the highest power that could be achieved while maintaining a stable molten zone. A higher power results in too large of a molten zone that cannot be supported by the surface tension of molten Cu_2O. The 58.8% power level represents an intermediate temperature.

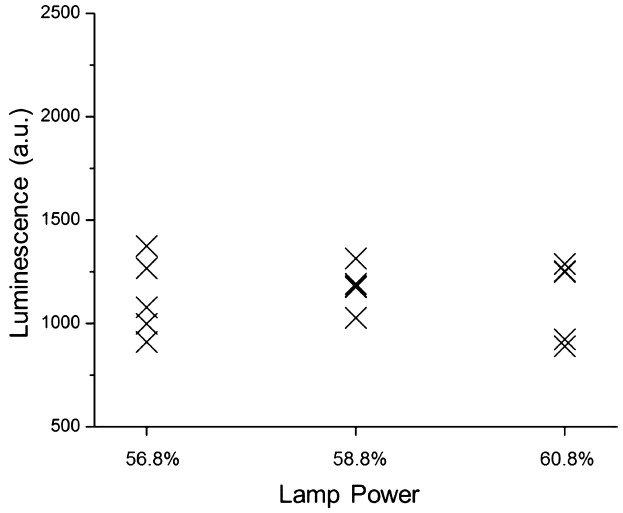

Figure 5. Copper vacancy luminescence for three Cu_2O crystals grown under different furnace lamp powers.

The temperature of the molten zone cannot be directly measured in the floating zone furnace used in this study. An increase in size of the molten zone between the lowest and highest power setting studied was observed. While the temperature of the crystal cannot be directly measured, the increase in size of the molten zone indicates that the temperature of the molten zone was increased. There was, however, no significant difference in the luminescence intensity

dx.doi.org/10.1021/cg401081m | Cryst. Growth Des. 2013, 13, 4914−4922

among the three samples. This result suggests that while the temperature of the molten zone was increased, the heating profile generated by the ellipsoidal mirrors is narrow enough that the temperature profile of the crystal below the molten zone was not changed enough to influence cuprous oxide oxidation kinetics. This result is consistent with the fact that as the lamp power is increased, the temperature gradient along the sample also increases.[47] In other words, the increase in temperature was more focused on the molten zone more than the solid above and below the molten zone, where oxidation to CuO would occur. If the oxidation kinetics were affected by the increased temperature, a change in copper vacancy luminescence should be observed. The fact that no change in luminescence was observed indicates that the amount of CuO precipitation and copper vacancy removal was not strongly affected.

3.6. Varying Growth Rate. A crystal was grown from a 99.9% pure copper rod 6.35 mm in diameter. The growth rate was varied incrementally during the course of crystal growth. The growth rates ranged from 3.5 to 17.5 mm/h and were changed after every 7 mm of growth with an increase of 3.5 mm/h per increment. The growth rate is therefore a function of position along the growth axis. The crystal was sliced along the growth axis, and photoluminescence was measured along the entire sample. Integrated copper vacancy photoluminescence for varying growth rates is plotted in Figure 6. The changes in

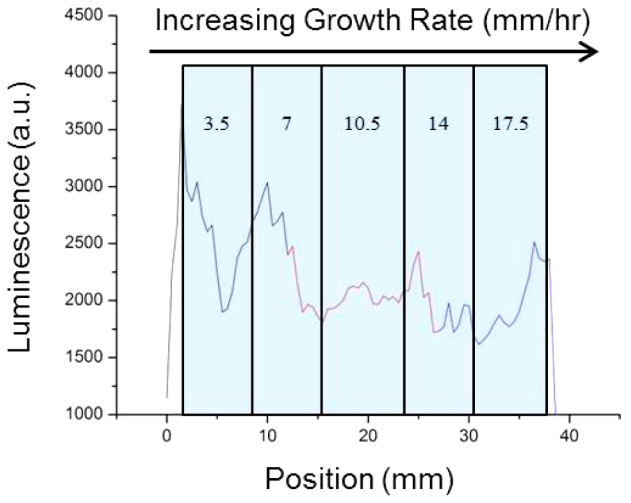

Figure 6. Copper vacancy luminescence along the growth axis of a single Cu_2O sample grown with incrementally increasing growth rates. Growth rates (mm/h) of crystal segments are labeled in blue boxes. The black, red, and blue coloring of the line represents the different segments of the same crystal from which the measurement was taken.

growth rates are labeled in blue boxes. No effect from varying growth rate on copper vacancy formation is observed. One may expect slower growth rates to allow more time for CuO formation to occur since the crystal directly below the molten zone would be at kinetically relevant temperatures for longer periods of time. This effect was previously observed by Ito et al.[41] They found that a slower growth rate reduced the number of copper vacancies.

This discrepancy between this work and results from Ito et al. is attributed to the difference in optical furnace design. The furnace used by Ito et al. consists of a single lamp, while this study uses a four lamp system. The four lamp system should provide a radially more uniform and axially narrower heating profile during crystal growth. A description of the four lamp system is provided elsewhere.[47] The difference in furnace design may explain why Ito et al. found that slower growth rates result in smaller copper vacancy concentrations. The narrower heating profile in a four mirror lamp system may reduce the extent to which the growth rates that were examined in this study affect CuO formation and copper vacancy removal.

3.7. Postgrowth Annealing. According to the reverse of eq 1, annealing crystals within the Cu_2O phase boundary should increase the number of copper vacancies as CuO inclusions are reduced to Cu_2O. The concentration of copper vacancies should be controlled through the amount of CuO formed in the bulk of the crystal as it is cooled. Quenched samples should therefore show an increase in copper vacancies, and samples cooled more slowly should show a reduction in copper vacancies when compared to the as-grown crystals.

The copper vacancy photoluminescence peak was measured several times for each of the nine annealed crystal slices. Integrated intensities are plotted as a function of annealing time in Figure 7. Blue and red points represent samples that were

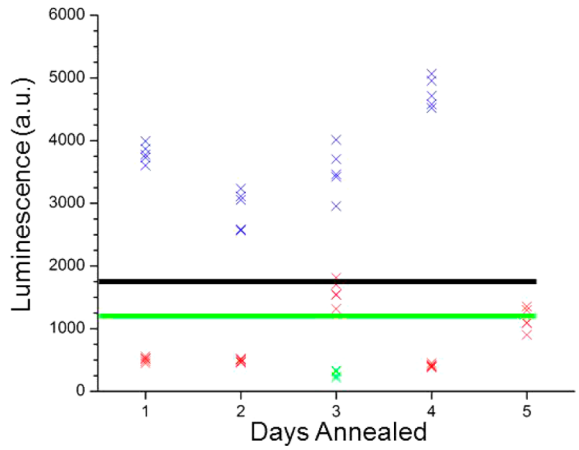

Figure 7. Copper vacancy luminescence for Cu_2O crystals annealed at 1045 °C at varying times. Blue points represent samples that were quenched to room temperature. Red and green points represent samples that were cooled at a rate of 5 °C/min to room temperature. Lines represent an average luminescence of samples that were not annealed. Samples from a 99.999% pure sample are colored green. All other samples were cut from the same 99.99% pure crystal.

quenched and cooled at 5 °C/min, respectively. The horizontal black line represents the average luminescence intensity of the control sample that was not annealed. All quenched samples contain higher copper vacancy concentrations and all 5 °C/min cooled samples contain fewer copper vacancies when compared to the as-grown crystal. The difference in the luminescence between the quenched and 5 °C/min cooled samples is approximately an order of magnitude. The samples that were cooled at 5 °C/min gave a narrower spread of the measured luminescence intensity than the samples that were quenched. This indicates that the samples cooled more slowly are more homogeneous than those quenched.

Annealing times longer than 1 day do not further reduce copper vacancies when samples are cooled at 5 °C/min. This indicates that the majority of the CuO is reduced to Cu_2O within 1 day. For this reason, the large spread of luminescence intensity in the quenched samples is not attributed to variation in annealing times. The large spread in luminescence intensity

dx.doi.org/10.1021/cg401081m | Cryst. Growth Des. 2013, 13, 4914−4922

among all the quenched samples is attributed to the inhomogeneity that results from rapid cooling. Samples cooled at 5 °C/min that were annealed for 3 and 5 days have higher vacancy concentrations and a greater spread of luminescence intensities than other slow cooled samples. This could result from variations in polishing depth or portion of the crystal from which the slice was cut. Despite these variations, all 5 °C/min cooled annealed samples show a reduction in copper vacancies.

An annealing experiment was performed on a high purity sample to determine if the number of copper vacancies can be further reduced by increasing the purity. The average photoluminescence from the crystal grown from 99.999% pure copper with otherwise identical growth conditions is shown as the horizontal green line in Figure 7. Three of the five annealed samples cooled at 5 °C/min contain fewer vacancies than the reference high purity sample. Photoluminescence measurements from the annealed high purity sample that was cooled at 5 °C/min are shown as green points in Figure 7. All points measured from this sample are lower in intensity than all points from the other annealed samples, indicating that superior results can be obtained by annealing a high purity sample.

The difference in copper vacancy concentrations between the high and low purity samples is significantly smaller for the annealed samples than the reference samples. This difference is explained by the fact that the annealed samples were cooled more slowly. Since the effect of purity on the number of copper vacancies is attributed to the difference in activation energy for CuO formation, longer oxidation time periods can provide additional time for the lower purity sample to reach (or approach) an equilibrium state, which is otherwise achieved more quickly for the high purity sample with a lower activation energy.

At this point, factors that can be used to engineer copper vacancy levels in cuprous oxide crystals during and after growth have been identified. The mechanism for the reduction of copper vacancies in all samples, however, inherently introduces CuO as a secondary phase. A slice of a crystal prior to annealing is shown in Figure 8a. Black inclusions are clearly visible that have been previously characterized to be CuO.[37] Figure 8b shows a magnification of the inclusions. The larger inclusions are more concentrated in the middle of the sample because the center of the sample cools more slowly, which allows CuO to grow into larger particles than the particles closer to the surface. It is therefore a challenge to engineer crystal growth while also maintaining a phase pure Cu_2O crystal.

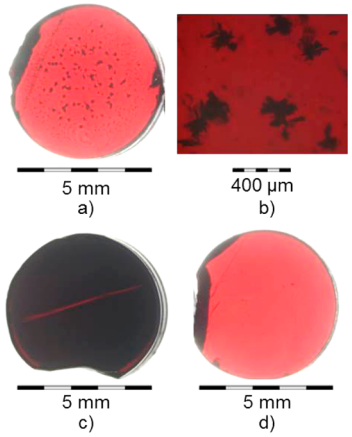

Figure 8. Photographs of three Cu_2O crystal slices cut from the same crystal. (a) A reference sample that was not annealed. (b) A magnification of the CuO inclusions. (c) A sample that was annealed at 1045 °C and quenched to room temperature. (d) A sample was annealed at 1045 °C and slow cooled at a rate of 5 °C/min to room temperature.

On the basis of the reverse of eq 1, the removal of CuO as a secondary phase and maximizing copper vacancies are achieved simultaneously. The formation of CuO upon cooling after annealing can be minimized or eliminated by reducing the amount of time the sample is in the CuO phase boundary at elevated temperatures. Figure 8c shows a sample that was quenched after annealing. This sample is more opaque than the reference sample. Since the sample was quenched from a temperature within the Cu_2O phase boundary and an increase in copper vacancies was observed, the amount of CuO in the sample should be minimal. A sample was analyzed via powder X-ray diffraction. The only peaks observed are from the Cu_2O phase, confirming that any CuO that did form is minimal. The powder pattern is provided in the Supporting Information (Figure S3). As the sample was quenched, small amounts of CuO quickly formed uniformly across the entire sample. While the amount of CuO formed is minimal, this uniform distribution of CuO would increase opacity. CuO formation can be avoided if the sample is cooled under a vacuum.[37]

Minimizing both CuO and copper vacancy formation cannot be simultaneously achieved based solely on eq 1. Preparation of a phase pure Cu_2O crystal with minimal copper vacancies is therefore challenging to achieve. Thin samples ($\leq$1 mm thick) that were annealed and cooled at 5 °C/min, however, contain minimal CuO inclusions, as seen in Figure 8d.

The mechanism for Cu_2O-CuO oxidation has been determined to be driven by copper migration from the center out toward the surface, expanding the CuO layer that initially forms on the surface.[11,12] Cooling samples more slowly will result in a greater amount of CuO precipitation. Vacancies provide a mechanism for CuO to form in the center of the sample without the need for the copper atom to reach the CuO surface layer. The CuO surface energy would be minimized, however, if the CuO formed through eq 1 sintered with the surface layer. Since copper vacancies diffuse through copper migration, cooling more slowly allows more time for vacancies to reach the surface and form CuO on the surface to minimize the CuO surface energy. When samples are cooled more rapidly, there is not enough time to allow for copper vacancies to reach the surface layer. Instead, CuO precipitates throughout the sample. The CuO surface layer can then be removed mechanically through polishing. CuO inclusions and copper vacancies can be simultaneously minimized through this process.

This method is only possible, however, with thin samples. Larger crystals with lower surface to volume ratios still have CuO inclusions after annealing because the inner portions of the samples will cool more slowly than the surface. Figure 9a shows a crystal prior to annealing that is approximately 2 cm long, and Figure 9b shows another crystal approximately 2 cm long after annealing for 5 days at 1045 °C and cooled at a rate of 5 °C/min. There is a clear reduction in the number of black inclusions after annealing. Black inclusions are still visible after annealing, however, in the center of the crystal. In thicker samples, CuO will nucleate and grow in the center of the sample rather than at the surface, as evidenced in Figures 8a and 9. This explains why crystals grown in the floating zone

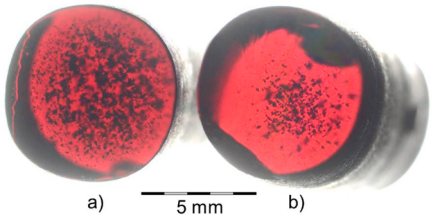

Figure 9. Photographs of Cu_2O crystals approximately 2 cm long. (a) An as-grown crystal. (b) A crystal that was annealed for 5 days followed by cooling to room temperature at a rate of 5 °C/min.

furnace initially contain CuO inclusions. The radial distance between the crystal surface to the region where the black inclusions are concentrated after annealing should dictate the maximum crystal thickness that can be used to prevent CuO inclusions from forming. On the basis of Figure 9b, crystal slices should be approximately 2 mm or thinner when a cooling rate of 5 °C/min is used.

4. CONCLUSIONS

A number of factors that affect floating zone crystal growth have been examined for their effects on the formation of copper vacancies. Two methodologies to reduce copper vacancies were considered. The first was to influence the amount of excess oxygen in the entire sample by varying the stoichiometry of the initial feed rod and by changing the rotation rate. Neither of these factors, however, affects the number of copper vacancies in the crystals. Additionally, single crystals can be grown using relatively rapid growth rates in a four lamp optical floating zone furnace without affecting the number of copper vacancies.

Copper vacancy reduction was instead facilitated through a second methodology by promoting precipitation of CuO. This strategy is counterintuitive as it inherently introduces a secondary phase; traditional procedures for obtaining Cu_2O crystals take precautions to specifically avoid the formation of CuO by cooling under a vacuum or using an inert atmosphere.[20,33,37,39,40] Promoting the formation of CuO, however, through the use of higher purity starting materials and growing under slightly oxidizing conditions, actually results in fewer copper vacancies. Higher purity samples contained fewer copper vacancies because impurities can raise the activation energy of Cu_2O oxidation. An oxidizing atmosphere promotes formation of CuO by increasing the temperature of the Cu_2O-CuO phase boundary. While this strategy inherently introduces CuO as a secondary phase, both CuO and copper vacancies can be simultaneously removed by annealing a thin sample in the Cu_2O phase boundary followed by cooling at 5 °C/min in air. A superior sample for exciton studies can be achieved by annealing a crystal slice made from higher purity starting material.

■ ASSOCIATED CONTENT

Supporting Information

Sample luminescence spectrum of a Cu_2O crystal, power dependence copper vacancy luminescence, and powder X-ray diffraction pattern of a crystal slice that was annealed at 1045 °C and quenched to room temperature. This material is available free of charge via the Internet at http://pubs.acs.org.

■ AUTHOR INFORMATION

Corresponding Author

*Phone: 847-491-3505. E-mail: krp@northwestern.edu.

Present Address

#(J.J.S.) Divison of Science, Mathematics, and Computing, Bard College at Simon's Rock, 84 Alford Road, Great Barrington, MA 01230.

Notes

The authors declare no competing financial interest.

■ ACKNOWLEDGMENTS

The authors thank Alexandre Revcolevschi for helpful discussions. Crystal growth was supported by NSF DMR-1307698 and in part by Argonne National Laboratory under U.S. Department of Energy contract DE-AC02-06CH11357. Optical measurements were supported by NSF IGERT DGE-0801685. K.C. was supported as part of the Center for Inverse Design, an Energy Frontier Research Center funded by the U.S. Department of Energy, Office of Science, Office of Basic Energy Sciences, under award number DE-AC-36-08GO28308. This work made use of the J. B. Cohen X-Ray Diffraction Facility and Optical Microscopy and Metallography Facility supported by the MRSEC program of the National Science Foundation (DMR-1121262) at the Materials Research Center of Northwestern University.

■ REFERENCES

(1) Raebiger, H.; Lany, S.; Zunger, A. *Phys. Rev. B* **2007**, *76*, 045209.
(2) Anderson, J. S.; Greenwood, N. N. *Proc. R. Soc. London, Ser. A* **1952**, *215*, 353.
(3) Wagner, C.; Hammen, H. *Z. Phys. Chem., Abt. B* **1938**, *40*, 197.
(4) Porat, O. *Solid State Ionics* **1994**, *74*, 229.
(5) O'Keeffe, M.; Moore, W. J. *J. Chem. Phys.* **1961**, *35*, 1324.
(6) Toth, R. S.; Kilkson, R.; Trivich, D. *Phys. Rev.* **1961**, *122*, 482.
(7) Ochin, P.; Petot, C.; Petotervas, G. *Solid State Ionics* **1984**, *12*, 135.
(8) Porat, O.; Riess, I. *Solid State Ionics* **1995**, *81*, 29.
(9) Bardeen, J.; Brattain, W. H.; Shockley, W. *J. Chem. Phys.* **1946**, *14*, 714.
(10) Moore, W. J.; Selikson, B. *J. Chem. Phys.* **1951**, *19*, 1539.
(11) Zhu, Y.; Mimura, K.; Isshiki, M. *Oxid. Met.* **2004**, *62*, 207.
(12) Grzesik, Z.; Migdalska, M. *High Temp. Mater. Processes* **2011**, *30*, 277.
(13) Mysyrowicz, A.; Hulin, D.; Antonetti, A. *Phys. Rev. Lett.* **1979**, *43*, 1123.
(14) Peterson, N. L.; Wiley, C. L. *J. Phys. Chem. Solids* **1984**, *45*, 281.
(15) Sui, Y.; Fu, W.; Yang, H.; Zeng, Y.; Zhang, Y.; Zhao, Q.; Li, Y.; Zhou, X.; Leng, Y.; Li, M.; Zou, G. *Cryst. Growth Des.* **2010**, *10*, 99.
(16) Zhang, Y.; Deng, B.; Zhang, T.; Gao, D.; Xu, A.-W. *J. Phys. Chem. C* **2010**, *114*, 5073.
(17) Lan, X.; Zhang, J.; Gao, H.; Wang, T. *CrystEngComm* **2011**, *13*, 633.
(18) Valodkar, M.; Pal, A.; Thakore, S. *J. Alloys Compd.* **2011**, *509*, 523.
(19) Toth, R. S.; Kilkson, R.; Trivich, D. *J. Appl. Phys.* **1960**, *31*, 1117.
(20) Mani, S.; Jang, J. I.; Ketterson, J. B.; Park, H. Y. *J. Cryst. Growth* **2009**, *311*, 3549.
(21) Naka, N.; Hashimoto, S.; Ishihara, T. *Jpn. J. Appl. Phys., Part 1* **2005**, *44*, 5096.
(22) Yin, Z. G.; Zhang, H. T.; Goodner, D. M.; Bedzyk, M. J.; Chang, R. P. H.; Sun, Y.; Ketterson, J. B. *Appl. Phys. Lett.* **2005**, *86*, 061901.
(23) Markworth, P. R.; Chang, R. P. H.; Sun, Y.; Wong, G. K.; Ketterson, J. B. *J. Mater. Res.* **2001**, *16*, 914.
(24) Dold, P.; Barz, A.; Recha, S.; Pressel, K.; Franz, M.; Benz, K. W. *J. Cryst. Growth* **1998**, *192*, 125.

(25) Harada, K.; Shimanuki, S.; Kobayashi, T.; Saitoh, S.; Yamashita, Y. *J. Am. Ceram. Soc.* **1998**, *81*, 2785.
(26) Isaenko, L.; Krinitsin, P.; Vedenyapin, V.; Yelisseyev, A.; Merkulov, A.; Zondy, J. J.; Petrov, V. *Cryst. Growth Des.* **2005**, *5*, 1325.
(27) Yang, G.; Jie, W.; Wang, T.; Li, G.; Li, W.; Hua, H. *Cryst. Growth Des.* **2007**, *7*, 435.
(28) Ikeda, T.; Marolf, N. J.; Snyder, G. J. *Cryst. Growth Des.* **2011**, *11*, 4183.
(29) Weber, M. J.; Bass, M.; Andringa, K.; Monchamp, R. R.; Comperch., E. *Appl. Phys. Lett.* **1969**, *15*, 342.
(30) Kitamura, K.; Yamamoto, J. K.; Iyi, N.; Kimura, S.; Hayashi, T. *J. Cryst. Growth* **1992**, *116*, 327.
(31) Bohm, J.; Heimann, R. B.; Hengst, M.; Roewer, R.; Schindler, J. *J. Cryst. Growth* **1999**, *204*, 128.
(32) Sabharwal, S. C.; Sangeeta; Desai, D. G. *Cryst. Growth Des.* **2006**, *6*, 58.
(33) Zucker, R. S. *J. Electrochem. Soc.* **1965**, *112*, 417.
(34) Koohpayeh, S. M.; Fort, D.; Abell, J. S. *Prog. Cryst. Growth Charact. Mater.* **2008**, *54*, 121.
(35) Dabkowska, H. A.; Dabkowski, A. B. In *Springer Handbook of Crystal Growth*; Dhanaraj, G. B., K.; Prasad, V.; Dudley, M., Eds.; Springer-Verlag Berlin Heidelberg: Berlin, Germany, 2010; p 367.
(36) O'Keeffe, M.; Moore, W. J. *J. Chem. Phys.* **1962**, *36*, 3009.
(37) Schmidt-Whitley, R. D.; Martinez-Clemente, M.; Revcolevschi, A. *J. Cryst. Growth* **1974**, *23*, 113.
(38) Trivich, D.; Pollack, G. P. *J. Electrochem. Soc.* **1970**, *117*, 344.
(39) Brower, W. S.; Parker, H. S. *J. Cryst. Growth* **1971**, *8*, 227.
(40) Loison, J. L.; Robino, M.; Schwab, C. *J. Cryst. Growth* **1980**, *50*, 816.
(41) Ito, T.; Yamaguchi, H.; Okabe, K.; Masumi, T. *J. Mater. Sci.* **1998**, *33*, 3555.
(42) Hauffe, K.; Kofstad, P. *Z. Elektrochem* **1955**, *59*, 399.
(43) Meijering, J. L.; Verheijke, M. L. *Acta Metall.* **1959**, *7*, 331.
(44) Bloem, J. *Philips Res. Rep.* **1958**, *13*, 167.
(45) Duvvury, C.; Kenway, D. J.; Weichman, F. L. *J. Lumin.* **1975**, *10*, 415.
(46) Ito, T.; Masumi, T. *J. Phys. Soc. Jpn.* **1997**, *66*, 2185.
(47) Koohpayeh, S. M.; Fort, D.; Bradshaw, A.; Abell, J. S. *J. Cryst. Growth* **2009**, *311*, 2513.